The Sizes of Life

E.W. Tekwa (edtekwa@gmail.com)
University of British Columbia https://orcid.org/0000-0003-2971-6128
Katrina Catalano
Rutgers, The State University of New Jersey
Anna Bazzicalupo
University of British Columbia
Mary O'Connor
University of British Columbia
Malin Pinsky
Rutgers, The State University of New Jersey https://orcid.org/0000-0002-8523-8952

Research Article

Keywords: Biomass, body size spectrum, complexity, macroecology, macroevolution, metabolic food web, marine, multicellularity, subterranean, terrestrial

Posted Date: October 19th, 2022

DOI: https://doi.org/10.21203/rs.3.rs-144241/v2

The Sizes of Life

E.W. Tekwa[1,2,3*], Katrina A. Catalano[3], Anna L. Bazzicalupo[1], Mary I. O'Connor[1], Malin L. Pinsky[3]

[1]Department of Zoology, University of British Columbia, Vancouver, BC, Canada.

[2]Hakai Institute, Heriot Bay, BC, Canada

[3]Department of Ecology, Evolution, and Natural Resources, Rutgers University, NJ, USA.

*Corresponding author, Email: ewtekwa@gmail.com, ORCID: 0000-0003-2971-6128

Author Contributions: ET and MP conceived the project, ET, KC and AB compiled the data, all authors designed the analyses, ET conducted analyses, and all authors contributed to writing.

Abstract

Recent research has revealed the diversity and biomass of life on Earth, but how that biomass is distributed across body sizes remains unclear. We compile the present-day global body size-biomass spectra for the terrestrial, marine, and subterranean realms. To achieve this compilation, we pair biomass estimates with previously uncatalogued body size ranges across all free-living biological groups. These data show that diverse organism types converge on similar overall minimum and maximum sizes. We then propagate biomass and size uncertainties and provide statistical descriptions of body size-biomass spectra across and within major habitat realms. Power laws show exponentially decreasing abundance (exponent -0.9, R^2=0.97) and nearly equal biomass (exponent 0.09, R^2=0.56) across log size bins. Gaussian mixture models show small and large organisms outweigh other sizes by about one order magnitude (R^2=0.86 in the size-biomass spectrum), but one-to-two orders of magnitude uncertainty persists across all organisms. The results show that the global body size-biomass relationships may be bimodal, but additional data will be needed to clarify whether global-scale universal constraints or local forces shape these patterns.

Keywords: Biomass, body size spectrum, complexity, macroecology, macroevolution, metabolic food web, marine, multicellularity, subterranean, terrestrial

Introduction

Body size is a widely used metric in biodiversity, ecological, and evolutionary sciences because it is understood to mechanistically link physical, physiological and demographic processes [1,2]. Organisms on Earth range from 10^{-17} (*Nanoarchaeum equitans*) to 10^{9} g (*Sequoiadendron giganteum*) in body size, estimated as carbon weight. Body size representations within various taxa have been a major focus in macroecology and biogeography. Such representations are called size spectra, with size-biomass spectra being the cumulative biomass of selected organisms distributed across body size classes, integrated over all individuals and taxa (i.e., not averaging over species). These spectra are also known as biomass size spectra, which are related to size-abundance or normalized size-biomass spectra where the response variable is a monotonic transformation of biomass [3]. Theories have attempted to predict and explain these patterns in terms of energy availability and transfer, species interactions, and metabolic scaling [4–6]. Such theories have been particularly successful within limited taxonomic ranges, especially for the relationships between body size and abundance in terrestrial mammalian herbivores [7], marine phytoplankton [8], cross-realm producers [9], and marine trophic communities [10]. Within groups that share an energy source (not necessarily with trophic links), energetic equivalence (equal energetic availability to all populations) leads to a power law exponent of -0.75 for size-abundance or size-normalized biomass spectra (where biomass is divided by the size class or bin width), or an exponent of 0.25 for size-biomass spectra [7,11,12]. Across trophic levels, reduced energy transfer can lead to a power law exponent of -1 for size-abundance or size-normalized biomass spectra, or an exponent of 0 for size-biomass spectra [13]. Beyond fundamental science, the power law exponents have also been considered as indices of productivity among marine ecosystems [14]. Deviations from expected exponents can be used to understand perturbations to ecosystems, such as inferring changing food web structure and fish biomass due to fishing [3,15–17], or inferring changes to the real breadth of the energetic base in coral reef systems [18]. Thus, size spectra are keys to understanding biological and anthropogenic constraints to life within biological communities.

Still, questions remain about whether small, medium, or large organisms dominate standing biomass of life on Earth at the global scale [11,17,19]. Different disciplines have proposed different

biomass modes with or without reference to power laws. From a microbiology perspective, microbes dominate [20]; from the marine perspective, medium-sized plankton dominate [21]; and from the terrestrial perspective, large plants dominate [22]. Each has a legitimate claim based on analysis of particular ecosystems or sets of taxa, but these approaches also prevent a different and novel synthesis in which traditionally excluded organisms may fit in. Empirical studies of size-biomass relationships have yet to include both terrestrial producers and consumers, or both small and large marine producers. The common phrase of bacteria-to-whale, meant to convey a complete marine size range [2,3,21], actually leaves out seagrass, hard corals, and mangroves that have maximum sizes near that of blue whales and much greater biomass than marine mammals and yet are problematic in terms of body size definitions and mixed ecological roles. Increased inclusivity could violate previous theoretical assumptions of size-structured trophic communities that led to power law predictions. But macroecological power laws themselves first arose from empirical relationships [7,10,23,24], which only later inspired still-evolving theoretical explanations [6,25]. The fact that some organisms, habitats, and parts of biological materials are routinely excluded from macroecology suggests these entities are poorly understood and a larger picture is missing. Revealing global patterns is a key step towards understanding universal constraints. For example, metabolic and biochemical theories predict universal constraints that govern how biological rates vary with body size and temperature across all organisms, which are largely independent of between-organism interactions and habitat variations [25,26]. Inspiring and testing theories on biomass distributions at biome scales will depend on assessing the current state of living things, but this empirical exercise has so far been prevented by a lack of data synthesis on body size itself.

Our objective here is to compile the first global and taxonomically inclusive size-biomass spectra of present-day terrestrial, marine, and subterranean realms. Specifically, we compile for the first time data on body size range within major biological groups that include all free-living organisms. We then offer statistical descriptions of the global and habitat realm-specific spectra and their uncertainties. Statistical tests will focus on pattern detection rather than on previous theoretical hypotheses because these do not directly apply to global size-biomass spectra. Both the methodology of size spectra construction and statistical analyses serve as guides for how to integrate a taxonomically inclusive set of data with substantial uncertainties. The resulting catalogue of biomass data matched to body sizes stands as a

record of present knowledge about life on Earth. We then focus on assessing the quality of available data in order to guide future research on causal mechanisms.

Results

The body sizes (Table 1-Table 3) that comprise the most biomass on Earth are the small (mainly bacteria and archaea, 10^{-15} g per individual) and the large (mainly plants, 10^{7} g), and these peaks (15 Gt and 65 Gt) outweighed intermediate sizes (10^{-11} g to 10^{-2} g, ~1 Gt) by an order of magnitude (Figure 1A). The pattern is particularly clear on a linear biomass scale (Figure 1B). Biomass uncertainty persisted across all sizes, with 95% confidence bounds being two orders of magnitude from the smallest size to about 10 g and about one order of magnitude at larger sizes. Multiple unrelated groups exhibited similar upper size limits, including forest plants, grassland plants, fungi, wild terrestrial mammals, mangroves, fish, hard corals, seagrass, and marine mammals that contribute to the cumulative biomass peak at the size of 10^{7} g. All data and code are provided on https://github.com/edwardtekwa/BodySizeBiomass.

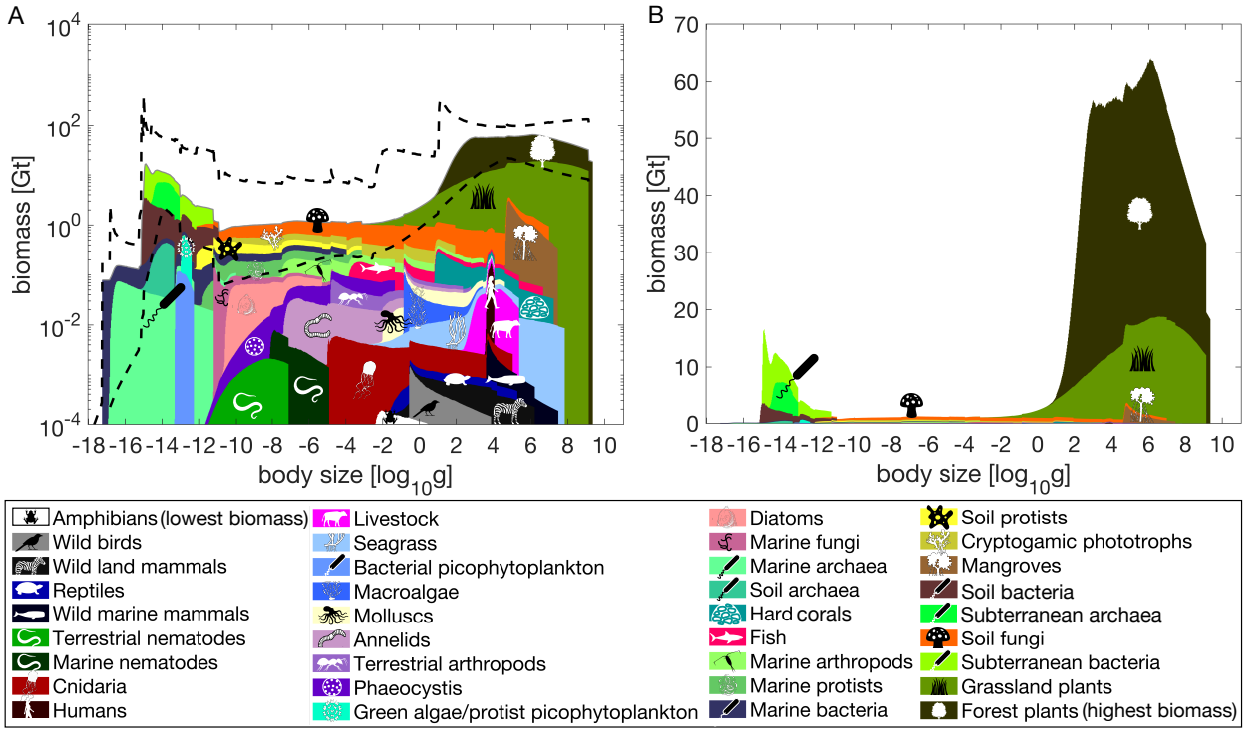

Figure 1. Global body size biomass spectrum. A. Median carbon biomass (log scale) as a function of body size with 95% confidence bounds (black dotted curves) for the across-group aggregate from 1000 bootstraps over within-group biomass and body size error distributions. Groups were organized from the least massive at the bottom to the most massive at the top for visibility on the log scale (see color legend for group identity). Thus, the height of groups at the bottom represents less biomass than an equal height of groups at the top. See Table **1**-Table 3 for within-group biomass uncertainties, and Table S3; for icon sources. **B**. Median biomass in linear biomass scale. Confidence bounds are not shown here because they are so large as to obscure the median patterns on the linear scale.

Table 1. Terrestrial body sizes and biomasses. º indicates spherical bodies formula (**[41]** for microbes), and ^ indicates tubular bodies formula (**[42]** for microbes). Biomass and uncertainty are from **[27]** unless indicated.

Group	Smallest	Largest	Min. body size (g C)	Median body size (g C)	Max. body size (g C)	Biomass (Gt C)	Uncertainty (fold)
Producers							
Forest plants	*Salix herbacea*º	*Sequoiadendron giganteum*	1.08E+01 [62,63]	1.13E+06	2.24E+09 [64]	337.5 [62]	1.2
Grassland plants	*Mibora minima*	*Holcus mollis*	3.75E-03 [65]	4.32E+06	1.34E+09 [62]	112.5 [62]	1.2
Cryptogamic phototrophs	*Nostoc punctiforme*	*Dawsonia superba*^	1.15E-11 [66]	2.72E-10*	8.75E+0 [68]	2.5†	2
Consumers							
Soil bacteria	*Actinobacteria spp.*º	*Proteobacteria spp.*º	7.37E-16 [70]	2.86E-14	1.15E-11 [70]	7.352	6
Soil archaea	*Crenarchaeota spp.*º	*Crenarchaeota spp.*º	7.37E-16 [70]	2.91E-14	4.72E-14 [70]	0.516	4
Soil protists	*Myamoeba spp.*º	*Dictyamoeba spp.*º	3.19E+25 [71]	7.37E-13	5.03E-11 [72]	1.605	4
Soil fungi	*Batrachochytrium dendrohabditis*º	*Armillaria ostoyae*	7.37E-13 [73]	1.53E-11	9.70E+06 [74]	11.802	3
Terrestrial arthropods	*Archegozetes longisetosus*	*Birgus latro*	1.50 E-5 [75]	2.00E-04	6.00E+02 [76]	0.212	15
Humans	*Homo sapiens*	*Homo sapiens*	3.75E+3 [77]	8.13E+03	1.13E+04 [77]	0.055	1.1
Livestock	*Gallus gallus domesticus*	*Bos taurus*	270 [27]	2.08E+04	2.25E+05 [27]	0.107	1.1
Wild land mammals	*Craseonycteris thonglongyai*	*Loxodonta africana*	0.038 [78]	2.53E+03	1.65E+06 [79]	0.003	4
Terrestrial nematodes	*Protohabditis hortulana*^	*Unspecified species*^	6.02E-13 [80]	5.00E-08	7.74E-08 [81]	0.002	10
Wild birds	*Mellisuga helenae*	*Struthio camelus*	0.27 [82]	6.67E+00	1.50E+04 [83]	0.199	10
Annelids	*Dendrobaena mammalis*^	*Microchaetus rappi*	4.16E-08[84]	2.59E-04	2.25E+02 [85]	0.006	10
Reptiles	*Brookseia spp.*	*Crocodylus porosus*	0.027 [86]	1.05E+02	1.80E+05 [87]	0.003	100
Amphibians	*Paedophryne amauensis*	*Andrias davidianus*	0.003 [88]	1.00E+00	7.50E+03 [89]	0.001‡	100

* Among lichens, likely the most abundant among cryptogams, we estimate that 87% contain phycobionts (*Trebouxia* 8-21 μm)[67] and 13% contain cyanobionts (*Nostoc punctiforme* 5 μm) [66]. This composition was used to estimate the mean body size.

† The total lichen biomass and uncertainty were obtained from [28]; to obtain cryptogamic phototrophs' biomass, the fungal portion of lichen was subtracted out. Twenty percent of fungi species occur in lichens [69], so 20% of the total fungal biomass was subtracted from the lichen biomass to get the cryptogamic phototrophs' biomass.

‡ Assumes amphibian habitat area is mainly rainforest, 5.5011347×10^{12} m^2 [62], and 0.1 individual per m^2 (lower than [27]'s likely overestimate). Uncertainty is unknown, so copied from reptiles which is the taxon with the highest uncertainty.

98

99 **Table 2.** Marine body sizes. º indicates spherical bodies formula ([41] for microbes). Biomass and
100 uncertainty are from [27] unless indicated.

101

Group	Smallest	Largest	Min. body size (g C)	Median body size (g C)	Max. body size (g C)	Biomass (Gt C)	Uncertainty (fold)
Producers							
Mangroves	*Rhizophora mangle*º *(dwarf)*	*Rhizophora mangle*º *(canopy)*	4.06E+04 [90]	6.49E+05*	2.88E+07 [90]	3.5 [31]	1.4
Seagrass	*Halophila decipiens*º	*Posidonia oceanica*º	2.63E-03 [92]	7.53E+04†	6.91E+07 [40,94]	0.11	10
Macroalgae	*Phaeophyceae spp.*	*Macrocystis pyrifera*	1.35E-01 [95,96]	2.00‡	2.70E+03 [95,96]	0.14	10
Bacterial picophytoplankton	*Prochlorococcus spp.*	-	5.00E-14 [97,98]	9.13E-14§	1.67E-13**	0.13	10
Green algae / protist picophyto-plankton	*Ostreococcus tauri*	-	1.05E-13 [97,99]	1.49E-13††	2.10E-13‡‡	0.30	10
Diatoms	*Thalassiosira pseudonana*	*Ethmodiscus spp.*	2.4E-11 [100]	9.08E-09§§	5.11E-06 [100]	0.31	10
Phaeocystis	*Phaeocystis globosa cell*º	*Phaeocystis globosa colony*º	1.15E-11 [101]	5.24E-04***	0.047 [101]	0.28	10
Consumers							
Marine bacteria	*Pelagibacter ubique*º	*Thiomargarita namibiensis*º	5.50 E-16 [102]	1.32E-14	1.10E-04 [103]	1.327	1.8
Marine archaea	*Nanoarchaeum equitans*	*Staphylothermus marinus*º	1.47E-17 [104]	1.22E-14	9.90E-11 [105]	0.332	3
Marine protists	*Picomonas judraskeda*º	*Rhizarian spp.*º	1.44E-12 [106]	2.26E-12	7.37E-04 [107]	1.058	10
Marine arthropods	*Stygotantulus Stocki*	*Homarus americanus*	3.537E-08 [75,76]	7.08E-06	3.00E+03 [108]	0.940	10
Fish	*Paedocypris progenetica*	*Rhincodon typus*	1.50E-04 [109]	6.27E-01	4.63E+06 [110]	0.668	8
Molluscs	*Ammonicera minortalis*	*Mesonychoteuthis hamiltoni*	0.01 [111,112]	4.02E-04	3.98E+04 [113–115]	0.182	10
Cnidaria	*Psammohydra nanna*	*Cyanea capillata*	1.00E-05 [116,117]	5.09E-03	1.00E+05 [116,118]	0.040	10
Hard corals	*Leptopsammia pruvoti*†††	*Porites lutea*	6.41 [29,119]	1.54E+03‡‡‡	1.68E+07 [121]	0.653§§§	4
Wild marine mammals	*Arctocephalus townsendi*	*Balaenoptera musculus*	4.05E+3 [122]	7.42E+04	2.99E+07 [110]	0.004	1.4
Marine nematodes	*Thalassomonhystera spp.*	*Platycomopsis spp.*	7.50E-09 [123]	1.80E-7[123]	1.20E-5 [123]	0.014	10
Marine fungi	*Malassezia restricta*	*Penicillium chrysogenum*	5.89E-12 [124,125]	1.39E-11	1.89E-05 [126]	0.325	10

* *Rhizophora mangle*, similar to estimates for other typical species [91]

† Based on genet size of *Zostera marina*, a widespread species [93] and carbon density [94].

‡ Based on *Laminaria saccharina*, a widespread species [96].

§ Diameter corresponds to definition of picophytoplanktons (2 µm), and corresponding carbon content is based on conversion formulae from the smallest species.

** Maximum sizes are estimated to correspond to the same deviation from the median size as minimum sizes are (on log scale).

†† Same method as for bacterial picophytoplankton.

‡‡ Same method as for bacterial picophytoplankton.

§§ Based on *Dactyliosolen fragilissimus* [100].

*** Mean size of colonies of *P. globosa* (2 mm) and *P. pouchetii* (1.5 mm), which are globally distributed and associated with bloom formation [101].

††† Classified as “generalist coral” for size estimate [30].

‡‡‡ Mean colony size was estimated as the geometric mean of corallite or maximum colony sizes. Only maximum colony sizes were found across species and may contain several genets, hence the geometric mean. For each estimate, measures for four coral types were converted first to cubic volumes using 3D morphologies, assuming branching morphotype for "competitive" and "weedy" corals, and massive morphotype for "generalist" and "stress-tolerant" corals [30]. Each volume estimates were then converted to mass using type-specific skeletal densities [120], C per $CaCO_3$, and weighted by global coral cover contributions [29].

§§§ Mean skeleton biomass was the geometric mean of two biomass estimates based on global coral cover having heights corresponding to either corallites or maximum colony sizes. Mean tissue biomass was 0.05 Gt with a 10 fold uncertainty [27]. Overall mean biomass was the sum of mean skeleton and tissue biomass, and overall uncertainty was obtained from assuming that the overall min/max correspond to the sum of min/max skeleton and tissue estimates.

Table 3. Subterranean consumer body sizes.

Group	Smallest body size	Largest body size	Min. body size (g C)	Median body size (g C)	Max. body size (g C)	Biomass (Gt C)	Uncertainty (fold)
Subterranean bacteria	*Proteobacteria spp.*	*Desulforudis audaxviator*	9.81E-16 [127]	2.1E-14 [32]	5.90E-12 [128]	18.9[*]	3[†]
Subterranean archaea	*Thermoproteus spp.*	*Miscellaneous Crenarchaeotal Group spp.*	2.49E-15 [130]	2.1E-14 [32]	9.22E-14 [131]	8.1[‡]	3[§]

Within-group size-biomass relationships reveal that five groups comprise most living biomass (Figure 2). Total biomass in the smallest size classes (<10^{-16} g) is dominated by marine bacteria (Figure 2AA). The biomass peak around 10^{-15} g is dominated by subterranean bacteria (Figure 2AH). Next, terrestrial fungi top the size range of 10^{-12} g to 1 g (Figure 2AG). Finally, grassland plants (1 g to 10 g, Figure 2GI) and forest plants (10 g to 10^{9} g, Figure 2GJ) make up almost all remaining biomass.

[*] Total subterranean microbial biomass was assumed to be the geometric mean of 23 to 31 PgC (which is 27 PgC) from [32]. 70% of microbial abundance is expected to be bacteria [129].

[†] Range of total subterranean microbial cell count from four models in [32] was 1.6 to 11.2 x 10^{29}, with a geometric mean of 4.2 x 10^{29}. This range corresponds to a three-fold uncertainty, which is similar to bacteria and archaea groups in other habitat realms.

[‡] 30% of microbial abundance is expected to be archaea [129]. See note for bacterial biomass.

[§] Same as uncertainty for subterranean bacteria.

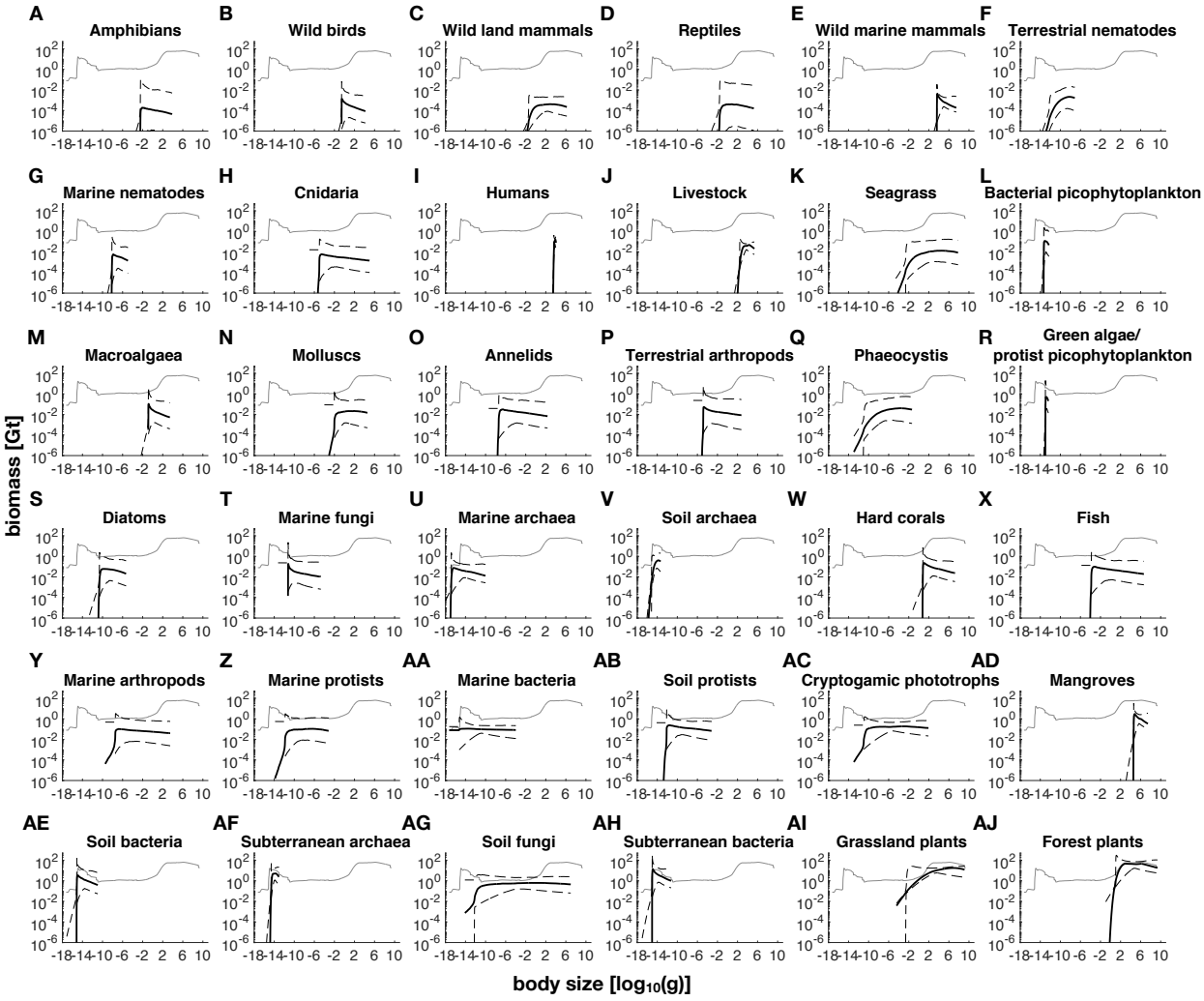

Figure 2. Body size biomass spectra within groups. Thick black curve is the median log biomass, and black dotted curves are 95% confidence bounds from 1000 resamples from within-group size and biomass uncertainties. Groups are organized from lowest to highest biomass (**A** to **AJ**). For reference, the thin grey curve is the median cumulative log biomass of all groups.

Terrestrial and marine spectra are different. Large body sizes dominate on land and across habitat realms, while the marine spectrum is roughly even across sizes (Figure 3). Marine organisms may only contribute significantly to the global biomass spectrum at the size range of 10^{-12} g to 10^{-3} g and below 10^{-16} g. Marine biomass is overall likely dwarfed by terrestrial and subterranean biomass, though there is

higher uncertainty in total biomass across size classes in the marine realm when compared to the terrestrial realm.

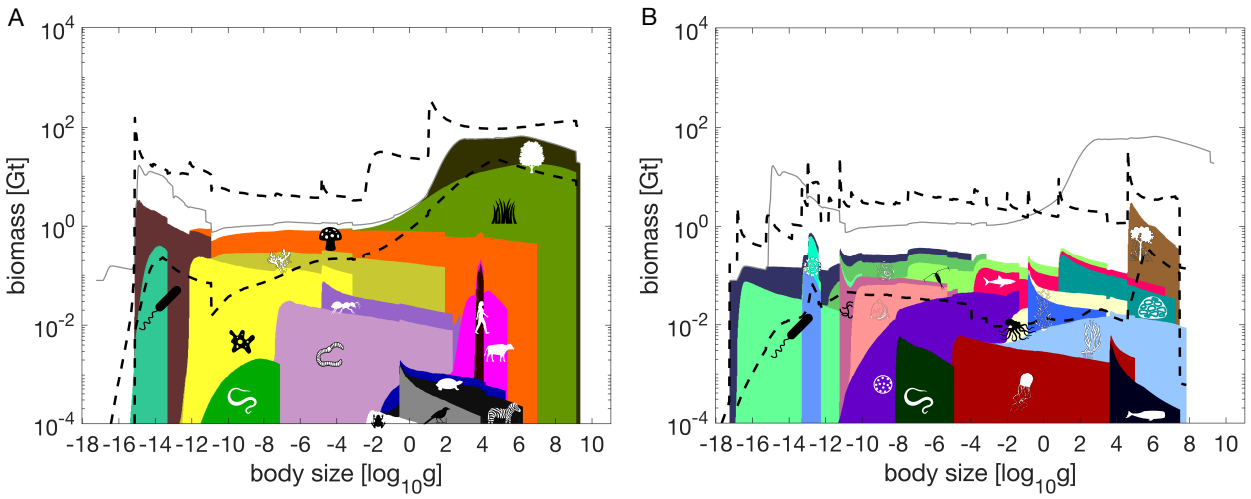

Figure 3. Body size biomass spectra by habitat realms. Median carbon biomass (log scale) as a function of body size with 95% confidence bounds (black dotted curves) for the across-group aggregate from 1000 bootstraps over within-group biomass and body size error distributions. For reference, the thin grey curve is the median cumulative log biomass of all groups. **A.** Terrestrial. **B.** Marine. Subterranean prokaryotes are excluded. See Figure 1 for color reference.

Linear regression of log biomass on log body size indicates a global power exponent β of 0.086±0.001 (s.d. across bootstraps) with a mean R^2 of 0.56 (Figure 4A). For the terrestrial realm, we obtained a similar β of 0.100±0.008 with a mean R^2 of 0.66 (Figure 4). These results show that biomass increases with size. Even though the variances explained are high, these power laws fail at the small size range, with confidence bounds missing the size class with the most biomass, filled by microbes. For the marine realm we obtained a much lower β of 0.019±0.005 with a mean R^2 of 0.11, indicating a similar biomass across log size bins.

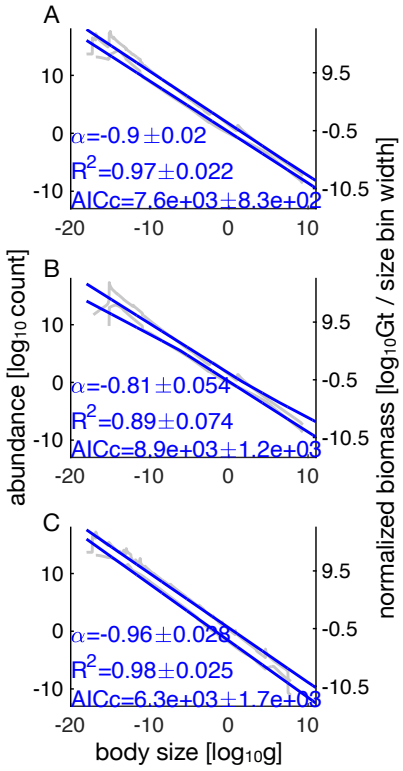

136

137 **Figure 4. Regression analyses on abundance.** Data is the same as in main text, except biomass is
138 replaced by abundance or normalized biomass (biomass divided by size class width). Rows represent
139 habitat realms (**A**: all realms, **B**: terrestrial, **C**: marine). Grey curves represent 95% confidence intervals of
140 the data, and blue curves represent 95% confidence intervals of the model from 1000 bootstraps. α is the
141 mean power exponent, and $\pm$ indicate standard deviations across bootstraps. Regression results are
142 identical whether it is performed on log abundance or log normalized biomass as the dependent variable,
143 because the latter is only offset from the former by a constant (-0.454).

144

145 The overall and terrestrial spectra show similar small mean power law exponents β (0.051 to
146 0.086 and 0.047 to 0.100 respectively), while the marine spectrum has an effectively zero β (-0.007 to
147 0.022) across choices of within group truncation methods, use of ramets instead of genets as body sizes,
148 and exclusion of metabolically inactive biomass like subterranean microbes (Table **4**, Fig. S3, Fig. S4). If
149 the linear regressions were performed on log size-log abundance instead (equivalent to normalized size-
150 biomass spectra), we would obtain exponents α of -0.90±0.02 (R^2=0.98), -0.80±0.05 (R^2=0.88), and -

0.96±0.03 (R^2=0.98), which are approximately β-1 as abundance is biomass divided by size (but not exactly because the data were directly transformed, not the mean exponents, Fig. S3). As the inflated R^2 suggest, the transformation from biomass to abundance may lead us to conclude that there is roughly equal biomass across all sizes (or slightly higher at large sizes on land), and there are little deviations visible from the power laws (Fig. S3). In comparison, the size-biomass spectra (Figure 5) are roughly detrended versions of size-abundance, with the -1 slope between size and abundance being the "trivial" trend on top of which both linear (power laws) and nonlinear (multimodal) patterns emerge.

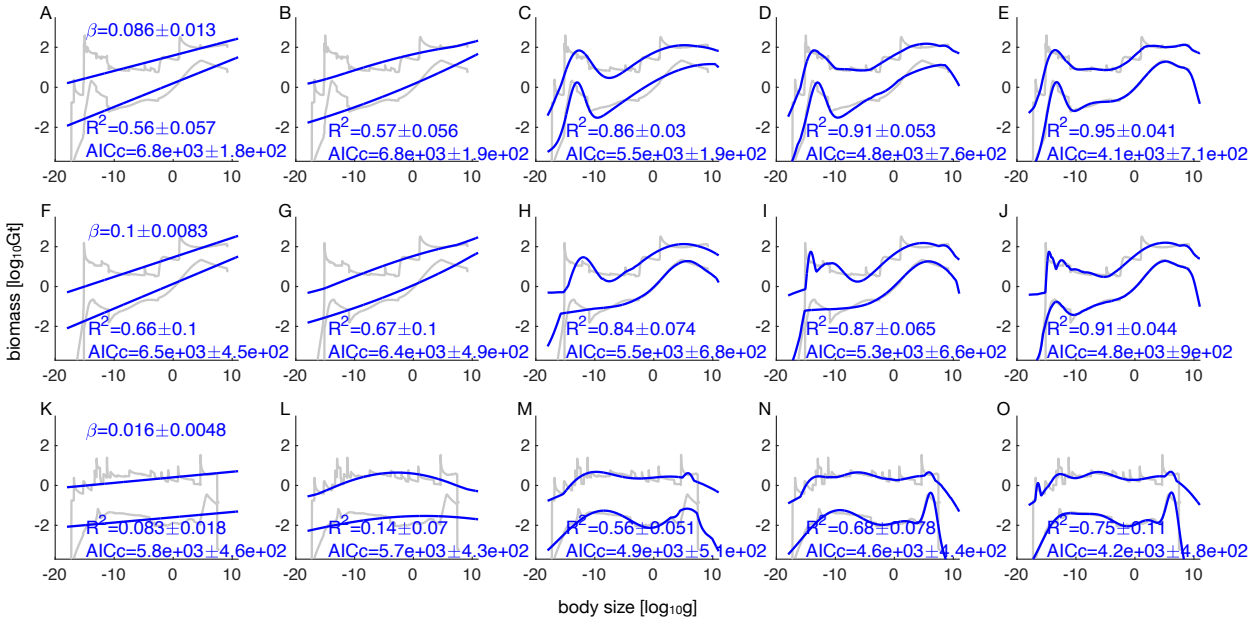

Figure 5. Regression analyses. Rows represent habitat realms (**A** to **E**: all realms, **F** to **J**: terrestrial, **K** to **O**: marine). Columns represent regression model types: (**A, F, K**: linear, **B, G, L**: Gaussian, **C, H, M**: Gaussian mixture 2, **D, I, N**: Gaussian mixture 3, **E, J, O**: Gaussian mixture 4). Grey curves represent 95% confidence intervals of the data, and blue curves represent 95% confidence intervals of the model from 1000 bootstraps. For linear models, regression slopes are mean power exponents ± standard deviations across bootstraps. R^2 and AICc scores are means ± standard deviations across 1000 bootstraps.

Table 4. Size-biomass power law exponents across realms and assumptions. Assumptions correspond to sensitive analyses plotted in Fig. S3. Exponents and R^2 result from 1000 bootstrapped linear regressions of log biomass on log size.

	β exponent (± bootstrap S.D.)	**R^2 (± bootstrap S.D.)**

Realm / Assumptions	***All***	***Terrestrial***	***Marine***	***All***	***Terrestrial***	***Marine***
A. All free-living, body size cutoff at -2/+0 $\log_{10}$g of reported (base model)	0.086±0.013	0.100±0.008	0.016±0.005	0.56±0.06	0.66±0.10	0.08±0.02
B. All free-living, body size cutoff at ±1 $\log_{10}$g of reported	0.082±0.007	0.079±0.007	0.019±0.005	0.40±0.08	0.45±0.11	0.05±0.03
C. All free-living, body size cutoff at ±0 $\log_{10}$g of reported	0.082±0.013	0.087±0.017	0.020±0.002	0.55±0.06	0.70±0.07	0.13±0.04
D. Ramet size definition, body size cutoff at -2/+0 $\log_{10}$g of reported	0.083±0.012	0.097±0.008	0.016±0.005	0.58±0.07	0.66±0.11	0.09±0.02
E. Metabolically active mass only, body size cutoff at -2/+0 $\log_{10}$g of reported	0.078±0.016	0.079±0.010	-0.009±0.006	0.68±0.09	0.58±0.13	0.05±0.03

Across terrestrial, marine, and subterranean (under both land and sea) organisms, there is a consistent $\log_{10}$ ratio of maximum to minimum size (size range) across all groups regardless of median size (slope=0, p=0.99), with a mean ratio of 7.0±4.2 (S.D.). In other words, as mean size increases, size range also increases with a power law exponent of 0 (Fig. S2). This supports the view that the non-normalized size-biomass spectra are an appropriate way to investigate representation across size, in addition to the statistical reasons outlined above.

Gaussian mixture models capable of multiple biomass modes reveal decreasing AICc scores with increasing number of Gaussian components overall and within realms, indicating better statistical descriptions than power laws (linear regressions) (Figure 5). However, visual inspection suggests the size-biomass relationships are well described by two mixture components, and further complexities appear hard to substantiate given the spectral uncertainty and variations in AICc across bootstraps (Figure 5C, H, M). These two-mode regressions explain much more of the data variation (R^2=0.86, 0.84, and 0.56 for all realms, terrestrial, and marine respectively) than power laws, the main difference being the ability to identify both small and large size-biomass modes. These results indicate two size modes are important and useful description of the global biomass spectra, beyond simple power laws.

Discussion

We performed a novel synthesis of the mass of all life in the biosphere, revealing size-biomass patterns that contain features reminiscent of published results, but also new features attributable to a greater taxonomic and error inclusion than previous efforts. Our three major biological findings were: 1.) lower and upper size limits were shared by diverse organisms and may contain most of the biomass on Earth; 2.) there was relatively consistent biomass across log body size classes, described by power law exponents near zero; and 3.) there was a greater proportion of total biomass on land concentrated in large organisms when compared to the ocean. Methodologically, we found that analyses relating log-biomass to log-size bins across all organisms (rather than size-abundance or normalized size-abundance), while retaining uncertainties in both size and biomass, revealed the most nuanced patterns.

The first pattern indicates universal lower and upper size limits. It is well-known that bacteria and archaea would share the lower size limit around 10^{-17} to 10^{-16} g. More surprisingly, multiple producer and consumer groups on land and in the sea coincide with maximum body sizes between 10^{7} and 10^{9} g – a relatively narrow range compared to the 26 orders of magnitude spanning all free-living things – including such diverse organisms as *Sequoiadendron giganteum, Holcus mollis, Armillaria ostoyae, Rhizophora mangleo, Posidonia oceanicao, Porites lutea*, and *Balaenoptera musculus*. This coincidence suggests an underlying upper size constraint [53,54]. Gaussian mixtures with two components describe size-biomass spectra better than power laws across-realm and within terrestrial and marine realms, suggesting that the lower and upper size limits across all free-living things are also modes where biomass is most concentrated. While our mean estimates indicate these modes contain roughly one order magnitude more biomass per log size than intermediate body sizes, uncertainty in biomass was consistently higher than this magnitude, indicating that the data is too poorly resolved to unequivocally support the bimodal pattern.

The second pattern indicates similar biomass across a large size range (a zero power law exponent explaining how biomass varies with body size). This is highly consistent with size spectra documented for aquatic ecosystems or within some taxonomic groups [7,10,12,25], which supports metabolic, competitive, and trophic explanations [13,25]. However, unlike previous studies, we included

214 microbes, large producers, and other traditionally excluded groups like corals and mangroves, and
215 propagated both biomass and size uncertainties. The fact that a near-zero exponent still persisted across
216 all habitat realms and analytical assumptions is surprising because our global-scale patterns are not likely
217 shaped by interactive forces such as trophic or competitive interactions previously proposed to cause
218 near-zero exponents [13]. We found some evidence for bimodality that diverged from power laws, but
219 large uncertainties prevent clear conclusions about such non-linear patterns.

220 The third finding, that biomass in the ocean is somewhat more evenly distributed across size
221 classes than on land offers clues to a future theoretical synthesis. The marine realm has a trophic
222 structure ordered by size, at least more so than on land and may thus conform closer to a trophic-
223 mediated uniform log-log size-biomass spectrum [17,25]. Biophysics and ecology – competition for light -
224 explain why primary producers are small in the ocean versus large on land [10,55,56]. However, this
225 narrative overlooks the striking similarities between the two realms. Large primary producers that also
226 provide physical structures to ecosystems dominate both land and sea (grass, tree, mangroves, corals,
227 seagrass and kelps) despite previous assertions. Despite their large biomass, however, we note that
228 large marine primary producers are restricted to shallow seas in which access to light and nutrients in the
229 sediment create a similar biophysical environment as on land, and do not dominate all marine
230 ecosystems (e.g., pelagic ecosystems). The causes of size-biomass differences in different habitat realms
231 remain to be explored.

232 Together, the findings of universal size limits possibly coinciding with a bimodal biomass
233 distribution, overall similar biomass across sizes, and differences between habitat realms suggest
234 possible roles for both universal and local explanations, depending on which feature of size-biomass
235 spectra we focus on. Previously unexplored universal constraints, perhaps similar to known biochemical
236 [26] or spatial-cellular mechanisms [57], can conceivably explain size limits and multiple high-biomass
237 modes at different sizes, but these constraints may be modified or overwritten by local interactions
238 between different organisms at finer spatial scales. The relative strengths of universal versus local
239 constraints may be partially understood by comparing size-biomass spectra and their uncertainties
240 across-realm versus within-realm. For instance, if the multiple modes observed across-realm are shared

by different realms, then spectral uncertainties should be lower across-realm because of more data (lower observation error and greater taxonomic coverage [58,59]) and universal constraints may be responsible. On the other hand, if different realms contribute different size modes, then spectral uncertainties should be higher for the across-realm spectrum because of higher biological variance, supporting the hypothesis that local constraints likely shape the across-realm pattern. However, this reduction in uncertainties at smaller scales is only detectable if sample coverage does not drastically decrease. In our analyses, some size modes coincide across all realms, leaving for the possibilities of both universal and local constraints. In addition, the across-realm data exhibits narrower confidence bounds and a stronger signal of bimodality than the terrestrial realm alone (Figure 5 C, H, M), and even more so when compared to the relatively hard-to-sample marine realm alone, because of higher aggregate data availability. These mode overlaps and uncertainty patterns indicate that universal constraints may strongly shape size-biomass spectra everywhere in similar ways, but this impression may also be due to a lack of data.

Our study shows that body size biomass spectra include substantial uncertainties. Within-group biomass uncertainties are high among some taxa, especially in microbes [27]. Definitions of body size (ramets vs. genets), mass (with vs. without metabolically inactive components like wood, skeleton, and subterranean microbes), and realm (mangroves being marine, terrestrial, or partial) remain open for debate. Sensitivity analyses on these variations show crude patterns like power laws are consistent, but nuances like the location of size-biomass peaks are uncertain. Our methodology was designed to minimize biases and propagated different sources of uncertainty. Indeed, this approach identified that large uncertainty persists through all sizes. In contrast, most previous macroecological studies have assumed certainty in minimum and maximum sizes instead of propagating size error. This assumption would have resulted in nearly uniform biomass distributions across log sizes within biological groups, which though did not affect mean power law parameter estimates, severely underestimated biomass uncertainty particularly at large sizes. Intuition tells us we are nowhere near as certain about where biomass is concentrated at large sizes (1.2 fold uncertainty at sizes 10 to 10^9 g assuming near-uniform within-group distributions in Fig. S3B, which is just the total biomass uncertainty for plants independent of size). Error propagations in both size and biomass are critical, resulting in ~10 fold uncertainty at the same size range (Figure 1). Given current knowledge on how size range varies with size within biological

groups and how biomass varies across sizes, we recommend studying the relationship between log-biomass and log-size (i.e. size-biomass spectra) using both power laws and non-linear statistics such as Gaussian mixtures. Our results highlight as much the current knowledge about the Earth's biosphere as it does potential gaps in observation. For instance, missing observations in specific size classes will tend to create an impression of multimodality even if in reality there is a continuum of biomass across sizes. Multiple within or between-study biomass estimates for particular biological groups may not be spatially independent and thus not representative, which can lead to an underestimation of uncertainty and bias in expected total biomass. However, we would not know what these uncertainties and biases are without more sampling. In light of these limitations, uncertainties of our knowledge of size-biomass spectra were likely underestimated, yet even these optimistic estimates reveal how little we know about our global biosphere. Quantifying uncertainties while identifying knowledge gaps remain priorities for macroecology [60].

The state and change of size-biomass spectra should be an urgent biodiversity assessment objective and a fertile ground for fundamental theories. The massive data requirement to conduct a more detailed spectral survey may resemble modern cosmology and its collaborative search for patterns in matter distribution [61]. Our results provide a first crude roadmap for what patterns may exist, but they will likely drastically change if size-biomass spectra become targets for research programs. To move forward, taxonomic inclusivity and a willingness to move beyond simple explanations would be required to document and understand our biosphere and anthropogenic change along the size gradient.

Materials and Methods

Biomass Data. To compile the global aggregate body size biomass spectrum among biological groups defined by habitat and taxonomy, we used global biomass (gigatons [Gt] in carbon content) assessments and minimum, median, and maximum body sizes (grams [g] in carbon content) within groups (Table 1-Table 3). We started with the most comprehensive existing synthesis of global biomass estimates, which incorporate uncertainties within and between multiple studies [27]. We followed the biological grouping in

Bar-On's database, which is not at a consistent taxonomic level but instead reflect the highest resolution at which a biomass estimate is available and comparable to other groups. Bar-On et al. drew from hundreds of studies that reported either biomass per sampled area or global extrapolations. The biomass per sampled area data was extrapolated by Bar-On et al. to the global scale based on the spatial distribution of environmental variables such as temperature and habitat type (akin to species distribution models but at a higher taxonomic level). The best estimates were obtained from the geometric mean of multiple data sources within group, and within- and between-study uncertainties were propagated (Fig. S1; see Bar-On et al.'s supplementary). We recognize that estimates of mean biomass and uncertainty can likely be improved for all groups, but this is not the main goal of our paper. Instead, we complemented Bar-On's database only when biological groups with potentially high biomass were missing or clearly outdated, including cryptogamic phototrophs [28], hard corals [29,30], mangroves [31], and subterranean prokaryotes [32,33]. Details for these new estimates are described in the footnotes of Table 1-Table 3. For some biological groups, new and potentially relevant data has appeared after Bar-On's publication. However, these studies cataloged only biomass by species without assessing their contributions to overall group biomass (e.g., bird [34] and mammals [35]), did not directly address present-day biomass (e.g., fish [36]), or were nearly identical to Bar-On's original estimates (e.g., terrestrial plants [37]). We included the plant woody material and coral skeleton produced by a living individual as part of biomass in our primary analysis, as was done in a previous global biomass synthesis [27]. This approach is consistent with the idea that all biomass regardless of metabolic status contributes to ecosystem functioning, though we also explored removing this biomass for sensitivity analyses and for future investigations.

Body Size Data. Size was defined as the carbon content (grams) of a unicellular or multicellular organism. Defining an organism is not entirely straightforward for clonal life forms like grasses, corals, and fungi. Here, we used genets as our primary definition but also explore alternatives in sensitivity analyses (presented in a later section). Genet is a widely accepted functional definition of a biological unit because genetically identical cell agglomerates function as coherent units and actively share resources, and often seem like separate organisms only because the connecting tissues are invisible to us above the substrate [38–40]. We collected minimum, median, and maximum genet sizes from a literature search

(Table 1-Table 3). Three points for biomass distribution within each group is minimalistic but, given our current knowledge of most groups, there are few other reliable size data to serve as additional reference points across each biological group. In the literature, mean sizes are often reported [27] while assuming a log-normal size-biomass distribution, so we can record these mean sizes as median size in our dataset without transformations. In cases where no mean sizes were reported, we used sizes mentioned in the literature as qualitatively representative species (those mentioned as most “common” or “widespread”), which are likely closer to the median rather than the mean size, given no a priori knowledge of the distribution. We used sizes at maturity because this is likely where biomass is concentrated within species [17], and because data are not available for most taxa on the contribution of spore or juvenile stages. However, our choices of body size cutoffs in subsequent estimates of within-group size-biomass spectra can approximate the biomass share of these immature sizes.

We converted all size observations to an estimate of mass in terms of carbon. The body sizes of some species were reported in units of grams carbon, but for many species we needed to extrapolate from wet or dry mass. When size estimates in the literature were reported in wet mass, we first searched the literature for a species-specific wet weight to grams carbon conversion. When a species-specific conversion was not available, we used the conversion from the closest relative within the taxon (see online repository tables). When taxon-specific conversions were not available, we assumed 30% dry mass per wet mass unit, and 50% carbon per dry mass unit following previous conventions [27]. In some cases, body size was reported in units of length (particularly among annelids, nematodes, and fishes). For these taxa, we found existing length to weight conversions for the species or the closest relative within the taxon. If body size was reported in diameter, as was the case for most unicellular species, we found the volume assuming that the organism was either spherical [41] or tubular [42], and then found existing biovolume to biomass conversions for the species or the closest relative within the taxon. For hard corals, since each corallite or colony is often tightly packed among other units, we estimated that volume as the cube of the reported diameter. While some of these assumptions may introduce size errors that we do not explicitly track in our uncertainty analyses, the different plausible conversion factors are within an order of magnitude. This error magnitude is much smaller than the size ranges estimated for each biological group based on the uncertainties that we did track (Fig. S2).

We excluded from our body size (dry carbon mass) any non-free-living disease organisms, which are mainly found within trematode, nematode, virus, bacterial, and fungal groups. Disease organisms tend to represent extreme body sizes within their groups and may have been double counted as host biomass, which present a special challenge to estimating within-group size-biomass distributions that we do not address here. It is likely that the total biomass of disease organisms is low both within hosts (3% or less) and together as a group (similar to wild birds, the second lowest biomass among free-living groups) [20,43] and thus should not appreciably affect the cross-taxa spectrum, even though parasites and microbiome-associated organisms may have disproportionate effects on the biomass of other organisms.

We assessed how a group's body mass range (as directly observed from data) is related to median body size as part of the size data exploration. We performed a linear regression of the ratio of $\log_{10}$ maximum size to log10 minimum size (from known species) on $\log_{10}$ median size across biological groups. A slope (power exponent) of 0 would indicate that the range of mass in terms of orders of magnitude is invariant with size class: that is, size range increases proportionally with median size. This scale invariance was assumed to be true in some size spectra theories that proposed log body size as the natural scale but was never tested [12]. A log size as the natural scale would also support the view that biomass plotted against log size does not need to be normalized (divided by size bin on linear scale), because then a log size bin at a larger size range does not *a priori* contain more organisms than a log size bin at a smaller size [11].

Within-Group Size-Biomass Spectra. We used the truncated generalized extreme value distribution to describe the body size-biomass distribution (with size on a log scale) within biological groups. The probability distribution function for biomass $y(x)$ was written in term of log size x, with B being the total biomass of the group, and the three parameters μ, σ, and ξ specifying the location, scale, and shape, respectively:

(1) $$y(x) = B\frac{1}{\sigma}t(z)^{\xi+1}\exp\left(-t(x)\right)$$

(2) $$t(x) = \begin{cases} \left(1+\xi\left(\frac{x-\mu}{\sigma}\right)\right)^{-1/\xi} & if\ \xi \neq 0 \\ exp\left(\frac{-(x-\mu)}{\sigma}\right) & if\ \xi = 0 \end{cases}$$

We chose this distribution because it is flexible, encompassing body size biomass relationships described before. Cross-taxa size-biomass relationships are often described in the literature using power laws, with log biomass linearly decreasing with log body size [11,16,44]. These functions implicitly assumed a minimum body size that is close to the most abundant (in terms of total biomass) body size. In addition, there is evidence that the size-biomass distribution becomes less consistently right-skewed as one descends into finer taxonomic classifications [17,45]. At the extreme, within many species ontogeny leads to a greater total biomass for large adults than for small larvae (left skew) [17]. The possibilities of both left and right skews makes a simple skewed distribution like the lognormal inappropriate. We used a truncated distribution to avoid the problem of long tails that would imply finite biomass at unrealistic body sizes, especially for groups with high total biomass (e.g., bacteria having finite biomass at the size of trees). We also renormalized the distribution to retain the total biomass under the curve.

Two steps were involved in generating a bootstrapped estimate of median size-biomass spectra per group. We first fit probability distributions (Eq. (1)) to three observed reference sizes for each organismal group compiled from the literature: minimum, median, and maximum sizes (Tables S1-S3). This fit was achieved by minimizing the sum of squares of the residuals between the three observed reference (log) sizes and the 0.05^{th}, 50^{th}, and 99.95^{th} percentiles of the truncated generalized extreme value distribution. The probability distribution thus placed close to 99.9% of the biomass within the reported size range. Truncation was applied at two orders of magnitude below the reported minimum size to accommodate uncertainties associated with undetected small species and immature individuals. This assumption is compatible with empirical evidence across marine and terrestrial life with offspring being around two orders of magnitude smaller than adults [46,47]. The upper size limits are likely more accurate than the lower size limits because larger species are easier to observe; in addition, the upper limits are not influenced by ontogeny, hence the asymmetry in truncation. We explored different truncation amounts to both lower and upper limits in sensitivity tests.

In the second step, we used the initial distribution fit from step one to represent our uncertainty in where the median biomass occurs within groups (Fig. S1). We resampled 1000 sets of these within-group median body size and biomass, keeping minimum and maximum sizes constant, and re-fit the truncated

generalized extreme value distribution each time to generate bootstrapped size-biomass relationships. This way, even in cases where biomass estimates have low uncertainty, such as in grassland plants, uncertainty in median size leads to large uncertainty in biomass at each possible grass size. In particular, to propagate median size uncertainty, the median size was randomly generated from the initially fitted truncated generalized distribution per bootstrap. To propagate biomass uncertainty, we randomly sampled in log space using standard deviation $\sigma = \lambda/1.96$, where the fold uncertainty correspond to the 95% confidence interval (with the log upper/lower bounds deviating by λ from the log mean) as reported in [27]. The 2.5th, 50th, and 97.5th percentiles of the bootstraps represent the lower bound, median, and upper bound of the within-group size-biomass spectra.

Statistical trends and modes across groups. Global median size-biomass spectra and confidence intervals were obtained by summing biomass density (Gt biomass per log body size) of all groups in a habitat realm (or realms) within each size bin (1/40 of a log unit) per bootstrap. Statistical descriptions were obtained for three different classifications of organisms: all realms, terrestrial, and marine.

To fit statistical relationships between size and cumulative biomass in each habitat realm, we did not perform simple regressions directly on the best estimated spectra because 1) biomass datapoints are not independent across sizes within groups, and 2) the cross-taxa biomass totals in any size class depends on all groups in that size class, making the error structure correlated across the size range. To obtain confidence bounds, we relied on a parametric bootstrapped ensemble of possible size class – total biomass spectra (size-biomass spectra). For each bootstrap, the possible continuous size-biomass spectrum is sampled 40 times per log size class from -18 to 11 in the same way that it was plotted for visualization (size bin width was 1/40 of a log unit). We then performed statistical regressions on each of the 1000 bootstrap sampled sets. The mean, 2.5th and 97.5th percentiles of the outputs represented each regression model's mean and 95% confidence bounds. Size bins with total biomass lower than 10^{-5} Gt (1000 t), which is an order of magnitude below the lower bound of amphibian biomass (the lowest among all groups), were not included as datapoints for the regression. A cutoff is necessary to avoid large or infinitely negative values after log transformation, which would prevent regression from proceeding.

We fit two kinds of regression models to test for trends in the amount of biomass across size classes across all taxa. For allometric power law relationships, ordinary least-squares regressions were performed to obtain power exponents β that explain the discrete sampled log size-log biomass (x-y) relationships. For Gaussian mixture models, up to four modes (components) were fit using an expectation maximization algorithm to minimize nonlinear least squares ('gauss1', 'gauss2', etc. in Matlab R2017a, MathWork, Natick, MA). During fitting for the Gaussian mixture, we added $\log_{10}(10^{-5})+1$ to log biomasses to ensure that the minimum value was 1; smaller values were already removed previously. For plotting, we subtracted $\log_{10}(10^{-5})+1$ from the solutions. We measured R^2 and the corrected Akaike Information Criterion (AICc) for model comparison [48], which results in means and standard deviations across bootstraps.

We performed the same regression analyses but with abundance in place of biomass, which is another traditional way to analyze size spectra [49] and as we will show is related to the normalized size-biomass spectra [11]. Abundance is calculated as biomass divided by body mass, so the power law exponent α for size (mass)-abundance is approximately the exponent for size (mass)-biomass minus one [3]. Additionally, the normalized size-biomass exponents were obtained by fitting power laws to total estimated biomass divided by the width of biomass size class. The width is a constant of one across the full range of sizes (biomass) observed in a continuous log spectrum, since each point along such a spectrum represents the biomass density, or biomass per log size unit. Consequently, normalized biomass B_N at log size x is $B_N=B/(10^{x+0.5}-10^{x-0.5})$ where B is the cumulative biomass density at x. With some arithmetic, we obtain $\log_{10}B_N=\log_{10}B-x-0.454$. Since $\log_{10}B-x$ is $\log_{10}(B/10^x)$, or $\log_{10}$(abundance), log normalized biomass in a continuous log spectrum is just log abundance minus 0.454. Thus, the power law exponent for the normalized size-biomass spectrum is identical to α. We compared the power exponents fitted for the size-abundance spectrum (α) and the size biomass spectrum (β) as alternative statistical descriptions of global size patterns.

Sensitivity Analyses. We repeat the regression analyses on global size-biomass spectra with datasets composed using different truncation limits for the within-group generalized extreme value distributions,

different definitions of body size (ramets vs. genets), and different mass inclusivity (with vs. without metabolically inactive material) (Fig. S3, S4, Table 1).

A lower truncation limit farther from median size leads to more weight toward juvenile biomass as discussed earlier. Truncations at maximum and minimum sizes resulted in uniform distributions.

The unit 'genets' was dissolved into smaller units of ramets for the variant definition of body size. Grassland plants, seagrass, soil fungi, and hard corals were affected by the switch to the ramet definition (Table S1). In particular, the original large size range for soil fungi was reduced but still remained the largest among all groups. This large size range reflects the group's unique history of having evolved and lost multicellularity many times [50], and having indeterminate growth through hyphae [51] that manifest in all possible sizes up to the upper limits.

We re-calculated the biomass spectrum only including the portion of the world's biomass that is "metabolically active", which would exclude skeletons, wood, and subterranean microbes [52]. This affects both the body size and biomass of forest plants, grassland plants, mangroves, and hard corals (Table S2).

Acknowledgements

The research was supported by the Tula Foundation; the Gordon and Betty Moore Foundation; MITACS; the Coral Reef Alliance; and NSF awards OCE-1426891, DEB-1616821, and OISE-1743711.

References

1. Bonner JT. The origins of multicellularity. Integrative Biology: Issues, News, and Reviews: Published in Association with The Society for Integrative and Comparative Biology. 1998;1: 27–36.

2. Andersen KH, Berge T, Gonçalves RJ, Hartvig M, Heuschele J, Hylander S, et al. Characteristic Sizes of Life in the Oceans, from Bacteria to Whales. Annual Review of Marine Science. 2016;8: 217–241. doi:10.1146/annurev-marine-122414-034144

3. Blanchard JL, Heneghan RF, Everett JD, Trebilco R, Richardson AJ. From Bacteria to Whales: Using Functional Size Spectra to Model Marine Ecosystems. Trends in Ecology & Evolution. 2017;32: 174–186. doi:10.1016/j.tree.2016.12.003

4. Brown JH. Macroecology. Chicago: University of Chicago Press; 1995.

5. Kerr SR, Dickie LM. The biomass spectrum: a predator-prey theory of aquatic production. New York: Columbia University Press; 2001.

6. West GB, Brown JH, Enquist BJ. A general model for ontogenetic growth. Nature. 2001;413: 628–631. doi:10.1038/35098076

7. Damuth J. Population density and body size in mammals. Nature. 1981;290: 699–700. doi:10.1038/290699a0

8. Li WKW. Macroecological patterns of phytoplankton in the northwestern North Atlantic Ocean. Nature. 2002;419: 154–157. doi:10.1038/nature00994

9. Belgrano A, Allen AP, Enquist BJ, Gillooly JF. Allometric scaling of maximum population density: a common rule for marine phytoplankton and terrestrial plants. Ecol Letters. 2002;5: 611–613. doi:10.1046/j.1461-0248.2002.00364.x

10. Sheldon RW, Prakash A, Sutcliffe WH. The size distribution of particles in the ocean. Limnol Oceanogr. 1972;17: 327–340. doi:10.4319/lo.1972.17.3.0327

11. Sprules WG, Barth LE. Surfing the biomass size spectrum: some remarks on history, theory, and application. Giacomini H, editor. Can J Fish Aquat Sci. 2016;73: 477–495. doi:10.1139/cjfas-2015-0115

12. Polishchuk LV. M.S. Ghilarov's Principle, or Biomass Equivalence Rule, as a Conservation Law in Ecology. Biol Bull Rev. 2019;9: 215–229. doi:10.1134/S2079086419030083

13. Jennings S, Oliveira JAAD, Warr KJ. Measurement of body size and abundance in tests of macroecological and food web theory. J Anim Ecology. 2007;76: 72–82. doi:10.1111/j.1365-2656.2006.01180.x

14. Jennings S, Blanchard JL. Fish abundance with no fishing: predictions based on macroecological theory. J Anim Ecology. 2004;73: 632–642. doi:10.1111/j.0021-8790.2004.00839.x

15. Shin Y-J, Rochet M-J, Jennings S, Field JG, Gislason H. Using size-based indicators to evaluate the ecosystem effects of fishing. ICES Journal of Marine Science. 2005;62: 384–396. doi:10.1016/j.icesjms.2005.01.004

16. Jennings S, Melin F, Blanchard JL, Forster RM, Dulvy NK, Wilson RW. Global-scale predictions of community and ecosystem properties from simple ecological theory. Proceedings of the Royal Society B: Biological Sciences. 2008;275: 1375–1383. doi:10.1098/rspb.2008.0192

17. Andersen KH, Jacobsen NS, Farnsworth KD. The theoretical foundations for size spectrum models of fish communities. Baum J, editor. Canadian Journal of Fisheries and Aquatic Sciences. 2016;73: 575–588. doi:10.1139/cjfas-2015-0230

18. Trebilco R, Baum JK, Salomon AK, Dulvy NK. Ecosystem ecology: size-based constraints on the pyramids of life. Trends in Ecology & Evolution. 2013;28: 423–431. doi:10.1016/j.tree.2013.03.008

19. Stock CA, Powell TM, Levin SA. Bottom–up and top–down forcing in a simple size-structured plankton dynamics model. Journal of Marine Systems. 2008;74: 134–152. doi:10.1016/j.jmarsys.2007.12.004

20. Whitman WB, Coleman DC, Wiebe WJ. Prokaryotes: The unseen majority. Proceedings of the National Academy of Sciences. 1998;95: 6578–6583. doi:10.1073/pnas.95.12.6578

21. Hatton IA, Heneghan RF, Bar-On YM, Galbraith ED. The global ocean size spectrum from bacteria to whales. Sci Adv. 2021;7: eabh3732. doi:10.1126/sciadv.abh3732

22. Erb K-H, Kastner T, Plutzar C, Bais ALS, Carvalhais N, Fetzel T, et al. Unexpectedly large impact of forest management and grazing on global vegetation biomass. Nature. 2017;553: 73–76. doi:10.1038/nature25138

23. Elton CS. Animal Ecology. New York, NY: Macmillan; 1927.

24. Barneche DR, Kulbicki M, Floeter SR, Friedlander AM, Allen AP. Energetic and ecological constraints on population density of reef fishes. Proc R Soc B. 2016;283: 20152186. doi:10.1098/rspb.2015.2186

25. Brown JH, Gillooly JF, Allen AP, Savage VM, West GB. Toward a metabolic theory of ecology. Ecology. 2004;85: 1771–1789. doi:10.1890/03-9000

26. Arroyo JI, Díez B, Kempes CP, West GB, Marquet PA. A general theory for temperature dependence in biology. Proc Natl Acad Sci USA. 2022;119: e2119872119. doi:10.1073/pnas.2119872119

27. Bar-On YM, Phillips R, Milo R. The biomass distribution on Earth. Proceedings of the National Academy of Sciences. 2018; 201711842. doi:10.1073/pnas.1711842115

28. Elbert W, Weber B, Burrows S, Steinkamp J, Büdel B, Andreae MO, et al. Contribution of cryptogamic covers to the global cycles of carbon and nitrogen. Nature Geoscience. 2012. doi:10.1038/ngeo1486

29. Darling ES, Alvarez-Filip L, Oliver TA, McClanahan TR, Côté IM. Evaluating life-history strategies of reef corals from species traits. Bellwood D, editor. Ecol Lett. 2012;15: 1378–1386. doi:10.1111/j.1461-0248.2012.01861.x

30. House JE, Brambilla V, Bidaut LM, Christie AP, Pizarro O, Madin JS, et al. Moving to 3D: Relationships between coral planar area, surface area and volume. PeerJ. 2018. doi:10.7717/peerj.4280

31. Hutchison J, Manica A, Swetnam R, Balmford A, Spalding M. Predicting Global Patterns in Mangrove Forest Biomass: Global patterns in mangrove biomass. Conservation Letters. 2014;7: 233–240. doi:10.1111/conl.12060

32. Magnabosco C, Lin L-H, Dong H, Bomberg M, Ghiorse W, Stan-Lotter H, et al. The biomass and biodiversity of the continental subsurface. Nature Geosci. 2018;11: 707–717. doi:10.1038/s41561-018-0221-6

33. Elhacham E, Ben-Uri L, Grozovski J, Bar-On YM, Milo R. Global human-made mass exceeds all living biomass. Nature. 2020;588: 442–444. doi:10.1038/s41586-020-3010-5

34. Callaghan CT, Nakagawa S, Cornwell WK. Global abundance estimates for 9,700 bird species. Proc Natl Acad Sci USA. 2021;118: e2023170118. doi:10.1073/pnas.2023170118

35. Santini L, Benítez-López A, Dormann CF, Huijbregts MAJ, Martins I. Population density estimates for terrestrial mammal species. Global Ecol Biogeogr. 2022;31: 978–994. doi:10.1111/geb.13476

36. Bianchi D, Carozza DA, Galbraith ED, Guiet J, DeVries T. Estimating global biomass and biogeochemical cycling of marine fish with and without fishing. Sci Adv. 2021;7: eabd7554. doi:10.1126/sciadv.abd7554

37. Ma H, Mo L, Crowther TW, Maynard DS, van den Hoogen J, Stocker BD, et al. The global distribution and environmental drivers of aboveground versus belowground plant biomass. Nat Ecol Evol. 2021;5: 1110–1122. doi:10.1038/s41559-021-01485-1

38. Heyward AJ, Collins JD. Fragmentation in Montipora ramosa: the genet and ramet concept applied to a reef coral. Coral Reefs. 1985;4: 35–40. doi:10.1007/BF00302202

39. Dahlberg A, Stenlid J. Size, distribution and biomass of genets in populations of Suillus bovinus (L.: Fr.) Roussel revealed by somatic incompatibility. New Phytologist. 1994. doi:10.1111/j.1469-8137.1994.tb04006.x

40. Arnaud-Haond S, Duarte CM, Diaz-Almela E, Marbà N, Sintes T, Serrão EA. Implications of extreme life span in clonal organisms: Millenary clones in meadows of the threatened seagrass posidonia oceanica. PLoS ONE. 2012. doi:10.1371/journal.pone.0030454

41. Fagerbakke KM, Norland S, Heldal M. The inorganic ion content of native aquatic bacteria. Canadian Journal of Microbiology. 1999. doi:10.1139/cjm-45-4-304

42. Eibye-Jacobsen D, Kristensen RM. A new genus and species of Dorvilleidae (Annelida, Polychaeta) from Bermuda, with a phylogenetic analysis of Dorvilleidae, Iphitimidae and Dinophilidae. Zoologica Scripta. 1994. doi:10.1111/j.1463-6409.1994.tb00379.x

43. Kuris AM, Hechinger RF, Shaw JC, Whitney KL, Aguirre-Macedo L, Boch CA, et al. Ecosystem energetic implications of parasite and free-living biomass in three estuaries. Nature. 2008;454: 515–518. doi:10.1038/nature06970

44. Guiet J, Poggiale J-C, Maury O. Modelling the community size-spectrum: recent developments and new directions. Ecological Modelling. 2016;337: 4–14. doi:10.1016/j.ecolmodel.2016.05.015

45. Kozlowski J, Gawelczyk AdamT. Why are species' body size distributions usually skewed to the right? Functional Ecology. 2002;16: 419–432. doi:10.1046/j.1365-2435.2002.00646.x

46. Neuheimer AB, Hartvig M, Heuschele J, Hylander S, Kiørboe T, Olsson KH, et al. Adult and offspring size in the ocean over 17 orders of magnitude follows two life history strategies. 2015;96: 9.

47. Meiri S. Endothermy, offspring size and evolution of parental provisioning in vertebrates. Biological Journal of the Linnean Society. 2019; blz138. doi:10.1093/biolinnean/blz138

48. Burnham KP, Anderson DR. Multimodel Inference: Understanding AIC and BIC in Model Selection. Sociological Methods & Research. 2004;33: 261–304. doi:10.1177/0049124104268644

49. White EP, Ernest SKM, Kerkhoff AJ, Enquist BJ. Relationships between body size and abundance in ecology. Trends in Ecology & Evolution. 2007;22: 323–330. doi:10.1016/j.tree.2007.03.007

50. Nagy LG, Kovács GM, Krizsán K. Complex multicellularity in fungi: evolutionary convergence, single origin, or both?: Complex multicellularity in Fungi. Biol Rev. 2018;93: 1778–1794. doi:10.1111/brv.12418

51. Dee JM, Mollicone M, Longcore JE, Roberson RW, Berbee ML. Cytology and molecular phylogenetics of Monoblepharidomycetes provide evidence for multiple independent origins of the hyphal habit in the Fungi. Mycologia. 2015. doi:10.3852/14-275

52. Pedersen K. Exploration of deep intraterrestrial microbial life: current perspectives. FEMS Microbiology Letters. 2000;185: 9–16. doi:10.1111/j.1574-6968.2000.tb09033.x

53. Blanckenhorn WU. The Evolution of Body Size: What Keeps Organisms Small? The Quarterly Review of Biology. 2000;75: 385–407. doi:10.1086/393620

54. Kingsolver JG, Pfennig DW. Individual-level selection as a cause of Cope's rule of phyletic size. Evolution. 2004;58: 1608–1612. doi:10.1111/j.0014-3820.2004.tb01740.x

55. May RM. Biological diversity: differences between land and sea. Phil Trans R Soc Lond B. 1994;343: 105–111. doi:10.1098/rstb.1994.0014

56. Potapov AM, Brose U, Scheu S, Tiunov AV. Trophic Position of Consumers and Size Structure of Food Webs across Aquatic and Terrestrial Ecosystems. The American Naturalist. 2019;194: 823–839. doi:10.1086/705811

57. Tekwa EW, Gonzalez A, Loreau M. Spatial evolutionary dynamics produce a negative cooperation–population size relationship. Theoretical Population Biology. 2019;125: 94–101. doi:10.1016/j.tpb.2018.12.003

612 58. Chao A. Nonparametric Estimation of the Number of Classes in a Population. Scandinavian Journal
613 of Statistics. 1984;11: 265–270.

614 59. Tekwa EW, Whalen MA, Martone PT, O'Connor MI. An improved species richness estimator using
615 spatial abundance data. bioRxiv; 2022. doi:10.1101/2022.05.02.490342

616 60. Bar-On YM, Milo R. Towards a quantitative view of the global ubiquity of biofilms. Nat Rev
617 Microbiol. 2019;17: 199–200. doi:10.1038/s41579-019-0162-0

618 61. Planck Collaboration, Ade PAR, Aghanim N, Arnaud M, Ashdown M, Aumont J, et al. Planck 2015
619 results: XIII. Cosmological parameters. A&A. 2016;594: A13. doi:10.1051/0004-6361/201525830

620 62. Erb KH, Kastner T, Plutzar C, Bais ALS, Carvalhais N, Fetzel T, et al. Unexpectedly large impact of
621 forest management and grazing on global vegetation biomass. Nature. 2018.
622 doi:10.1038/nature25138

623 63. Beerling DJ. Salix herbacea L. Journal of Ecology. 1998. doi:10.1046/j.1365-2745.1998.8650872.x

624 64. National Parks Service. Giant Sequoias. [cited 2 Oct 2020]. Available:
625 https://www.nps.gov/seki/learn/nature/bigtrees.htm

626 65. Pemadasa MA, Lovell PH. The Mineral Nutrition of Some Dune Annuals. The Journal of Ecology.
627 1974. doi:10.2307/2259004

628 66. Rippka R, Herdman M. Pasteur Culture Collection of Cyanobacterial Strains in Axenic Culture,
629 Catalogue and Taxonomic Handbook. Paris: Institut Pasteur; 1992.

630 67. Lutzoni F. Peltigera Project Overview. Available: http://lutzonilab.org/peltigera/overview/

631 68. Green TGA, Clayton-Greene KA. Studies on Dawsonia superba Grev. II. Growth rate. Journal of
632 Bryology. 1981. doi:10.1179/jbr.1981.11.4.723

633 69. Rikkinen J, Oksanen I, Lohtander K. Lichen guilds share related cyanobacterial symbionts. Science.
634 2002. doi:10.1126/science.1072961

635 70. Panikov NS. Contribution of nanosized bacteria to the total biomass and activity of a soil microbial
636 community. Advances in Applied Microbiology. 2005. doi:10.1016/S0065-2164(05)57008-4

637 71. Geisen S, Mitchell EAD, Adl S, Bonkowski M, Dunthorn M, Ekelund F, et al. Soil protists: A fertile
638 frontier in soil biology research. FEMS Microbiology Reviews. 2018. doi:10.1093/femsre/fuy006

639 72. Berney C, Geisen S, Van Wichelen J, Nitsche F, Vanormelingen P, Bonkowski M, et al. Expansion of
640 the "Reticulosphere": Diversity of Novel Branching and Network-forming Amoebae Helps to
641 Define Variosea (Amoebozoa). Protist. 2015. doi:10.1016/j.protis.2015.04.001

642 73. Global Invasive Species Database. Batrachochytrium dendrobatidis. Available:
643 http://www.iucngisd.org/gisd/species.php?sc=123

644 74. Smith ML, Bruhn JN, Anderson JB. The fungus Armillaria bulbosa is among the largest and oldest
645 living organisms. Nature. 1992. doi:10.1038/356428a0

646 75. Kawabata K, Urabe J. Length-weight relationships of eight freshwater planktonic crustacean species
647 in Japan. Freshwater Biology. 1998. doi:10.1046/j.1365-2427.1998.00267.x

648 76. Boxshall GA, Huys R. New Tantulocarid, Stygotantulus stocki, Parasitic on Harpacticoid Copepods,
649 with an Analysis of the Phylogenetic Relationships within the Maxillopoda. Journal of Crustacean
650 Biology. 1989. doi:10.2307/1548454

651 77. Walpole SC, Prieto-Merino D, Edwards P, Cleland J, Stevens G, Roberts I. The weight of nations: An
652 estimation of adult human biomass. BMC Public Health. 2012. doi:10.1186/1471-2458-12-439

653 78. Hill JE, Smith SE. Craseonycteris thonglongyai. Mammalian Species. 1981. doi:10.2307/3503984

654 79. Wood GL. The Guinness book of animal facts and feats. 3rd ed. Enfield, Middlesex: Guinness
655 Superlatives; 1982.

656 80. Abolafia J, Peña-Santiago R. Protorhabditis Hortulana Sp. N. (Rhabditida, Protorhabditidae) from
657 southern Iberian Peninsula, one of the smallest free-living soil nematodes known, with a
658 compendium of the genus. Zootaxa. 2016. doi:10.11646/zootaxa.4144.3.7

659 81. Mulder C, Vonk JA. Nematode traits and environmental constraints in 200 soil systems: Scaling
660 within the 60–6000 µm body size range. Ecology. 2011. doi:10.1890/11-0546.1

661 82. Blackburn TM, Gaston KJ. The Distribution of Body Sizes of the World's Bird Species. Oikos. 1994.
662 doi:10.2307/3545707

663 83. Nee S, Mooers A, Harvey PH. Tempo and mode of evolution revealed from molecular phylogenies.
664 Proceedings of the National Academy of Sciences of the United States of America. 1992.
665 doi:10.1073/pnas.89.17.8322

666 84. Hatton IA, Dobson AP, Storch D, Galbraith ED, Loreau M. Linking scaling laws across eukaryotes.
667 Proc Natl Acad Sci USA. 2019; 201900492. doi:10.1073/pnas.1900492116

668 85. Jim Pattison Group. Guinness World Records. New York; 1997.

669 86. Glaw F, Köhler J, Townsend TM, Vences M. Rivaling the world's smallest reptiles: Discovery of
670 miniaturized and microendemic new species of leaf chameleons (Brookesia) from northern
671 Madagascar. PLoS ONE. 2012. doi:10.1371/journal.pone.0031314

672 87. University of Michigan. Crocodylus porosus. In: Animal Diversity Web [Internet]. [cited 2 Oct 2020].
673 Available: https://animaldiversity.org/accounts/Crocodylus_porosus/

674 88. Rittmeyer EN, Allison A, Gründler MC, Thompson DK, Austin CC. Ecological guild evolution and the
675 discovery of the world's smallest vertebrate. PLoS ONE. 2012. doi:10.1371/journal.pone.0029797

89. Wang XM, Zhang KJ, Wang ZH, Ding YZ, Wu W, Huang S. The decline of the Chinese giant salamander Andrias davidianus and implications for its conservation. Oryx. 2004. doi:10.1017/S0030605304000341

90. Smithsonian Institution. Mangroves. [cited 1 Jul 2020]. Available: https://ocean.si.edu/ocean-life/plants-algae/mangroves

91. Njana MA, Meilby H, Eid T, Zahabu E, Malimbwi RE. Importance of tree basic density in biomass estimation and associated uncertainties: a case of three mangrove species in Tanzania. Annals of Forest Science. 2016. doi:10.1007/s13595-016-0583-0

92. Dawes C, Chan M, Chinn R, Koch EW, Lazar A, Tomasko D. Proximate composition, photosynthetic and respiratory responses of the seagrass Halophila engelmannii from Florida. Aquatic Botany. 1987. doi:10.1016/0304-3770(87)90067-2

93. De Witte LC, Stöcklin J. Longevity of clonal plants: Why it matters and how to measure it. Annals of Botany. 2010. doi:10.1093/aob/mcq191

94. Fourqurean JW, Duarte CM, Kennedy H, Marbà N, Holmer M, Mateo MA, et al. Seagrass ecosystems as a globally significant carbon stock. Nature Geoscience. 2012. doi:10.1038/ngeo1477

95. Catalina Island Marine Institute. Kelp: The Floating Forests. [cited 1 Jul 2020]. Available: https://cimioutdoored.org/kelp-forest/

96. Gevaert F, Davoult D, Creach A, Kling R, Janquin M-A, Seuront L, et al. Carbon and nitrogen content of Laminaria saccharina in the eastern English Channel: biometrics and seasonal variations . Journal of the Marine Biological Association of the United Kingdom. 2001. doi:10.1017/s0025315401004532

97. Mullin MM, Sloan PR, Eppley RW. Relationship between carbon content, cell volume, and area in phytoplankton. Limnology and Oceanography. 1966. doi:10.4319/lo.1966.11.2.0307

98. Partensky F, Hess WR, Vaulot D. Prochlorococcus, a marine photosynthetic prokaryote of global significance. Microbiology and molecular biology reviews : MMBR. 1999.

99. Palenik B, Grimwood J, Aerts A, Rouzé P, Salamov A, Putnam N, et al. The tiny eukaryote Ostreococcus provides genomic insights into the paradox of plankton speciation. Proceedings of the National Academy of Sciences of the United States of America. 2007. doi:10.1073/pnas.0611046104

100. Leblanc K, Arístegui J, Armand L, Assmy P, Beker B, Bode A, et al. A global diatom database- A bundance, biovolume and biomass in the world ocean. Earth System Science Data. 2012. doi:10.5194/essd-4-149-2012

101. Throndsen J. The Planktonic Marine Flagellates. Identifying Marine Phytoplankton. 1997. doi:10.1016/b978-012693018-4/50007-0

102. Rappé MS, Connon SA, Vergin KL, Giovannoni SJ. Cultivation of the ubiquitous SAR11 marine bacterioplankton clade. Nature. 2002. doi:10.1038/nature00917

103. Schulz HN, Brinkhoff T, Ferdelman TG, Hernández Mariné M, Teske A, Jørgensen BB. Dense populations of a giant sulfur bacterium in namibian shelf sediments. Science. 1999;284: 493–495. doi:10.1126/science.284.5413.493

104. Huber H, Hohn MJ, Rachel R, Fuchs T, Wimmer VC, Stetter KO. A new phylum of Archaea represented by a nanosized hyperthermophilic symbiont. Nature. 2002. doi:10.1038/417063a

105. Schulz HN, Jørgensen BB. Big Bacteria. Annual Review of Microbiology. 2001. doi:10.1146/annurev.micro.55.1.105

106. Moreira D, López-García P. The rise and fall of picobiliphytes: How assumed autotrophs turned out to be heterotrophs. BioEssays. 2014. doi:10.1002/bies.201300176

107. Biard T, Stemmann L, Picheral M, Mayot N, Vandromme P, Hauss H, et al. In situ imaging reveals the biomass of giant protists in the global ocean. Nature. 2016. doi:10.1038/nature17652

108. Jim Pattison Group. American lobster. Guiness World Records. New York; 1977.

109. FishBase. Schindleria brevipinguis. [cited 1 Sep 2020]. Available: https://www.fishbase.se/summary/Schindleria-brevipinguis.html

110. McClain CR, Balk MA, Benfield MC, Branch TA, Chen C, Cosgrove J, et al. Sizing ocean giants: Patterns of intraspecific size variation in marine megafauna. PeerJ. 2015. doi:10.7717/peerj.715

111. Páll-Gergely B, Hunyadi A, Jochum A, Asami T. Seven new hypselostomatid species from China, including some of the world's smallest land snails (Gastropoda, Pulmonata, Orthurethra). ZooKeys. 2015. doi:10.3897/zookeys.523.6114

112. Eckblad JW. Weight-Length Regression Models for Three Aquatic Gastropod Populations. American Midland Naturalist. 1971. doi:10.2307/2423940

113. Nilsson DE, Warrant EJ, Johnsen S, Hanlon R, Shashar N. A unique advantage for giant eyes in giant squid. Current Biology. 2012. doi:10.1016/j.cub.2012.02.031

114. The Official Website of the New Zealand Government. World's largest squid landed in NZ. Available: https://www.beehive.govt.nz/release/worlds-largest-squid-landed-nz

115. Eklöf J, Austin Å, Bergström U, Donadi S, Eriksson BDHK, Hansen J, et al. Size matters: Relationships between body size and body mass of common coastal, aquatic invertebrates in the Baltic Sea. PeerJ. 2017. doi:10.7717/peerj.2906

116. Pitt KA, Duarte CM, Lucas CH, Sutherland KR, Condon RH, Mianzan H, et al. Jellyfish Body Plans Provide Allometric Advantages beyond Low Carbon Content. PLoS ONE. 2013. doi:10.1371/journal.pone.0072683

117. Lucas CH, Pitt KA, Purcell JE, Lebrato M, Condon RH. What's in a jellyfish? Proximate and elemental composition and biometric relationships for use in biogeochemical studies. Ecology. 2011. doi:10.1890/11-0302.1

118. The Marine Life Information Network. Lion's mane jellyfish (Cyanea capillata). Available: https://www.marlin.ac.uk/species/detail/2090

119. Caroselli E, Zaccanti F, Mattioli G, Falini G, Levy O, Dubinsky Z, et al. Growth and demography of the solitary scleractinian coral Leptopsammia pruvoti along a sea surface temperature gradient in the mediterranean sea. PLoS ONE. 2012. doi:10.1371/journal.pone.0037848

120. Darling ES, McClanahan TR, Maina J, Gurney GG, Graham NAJ, Januchowski-Hartley F, et al. Social–environmental drivers inform strategic management of coral reefs in the Anthropocene. Nature Ecology and Evolution. 2019. doi:10.1038/s41559-019-0953-8

121. Brown DP, Basch L, Barshis D, Forsman Z, Fenner D, Goldberg J. American Samoa's island of giants: Massive Porites colonies at Ta'u island. Coral Reefs. 2009. doi:10.1007/s00338-009-0494-8

122. Belcher RL, Lee Jr. TE. Arctocephalus townsendi. Mammalian Species. 2002. doi:10.1644/1545-1410(2002)700<0001:at>2.0.co;2

123. Armenteros M, Ruiz-Abierno A. Body size distribution of free-living marine nematodes from a Caribbean coral reef. Nematology. 2015. doi:10.1163/15685411-00002930

124. Amend A. From Dandruff to Deep-Sea Vents: Malassezia-like Fungi Are Ecologically Hyper-diverse. PLoS Pathogens. 2014. doi:10.1371/journal.ppat.1004277

125. Wilson C, Nizet V, Maldonado Y, Remington J, Krupp MA, Klein J. Infectious Diseases of the Fetus and Newborn Infant. Infectious Diseases of the Fetus and Newborn Infant. 2011. doi:10.1016/C2009-0-50442-4

126. Aguilar-Trigueros CA, Rillig MC, Crowther TW. Applying allometric theory to fungi. ISME J. 2017;11: 2175–2180. doi:10.1038/ismej.2017.86

127. Wu X, Holmfeldt K, Hubalek V, Lundin D, Åström M, Bertilsson S, et al. Microbial metagenomes from three aquifers in the Fennoscandian shield terrestrial deep biosphere reveal metabolic partitioning among populations. ISME J. 2016;10: 1192–1203. doi:10.1038/ismej.2015.185

128. Abe S. Life Without the Sun. In: Astrobiology at NASA [Internet]. 10 Oct 2008. Available: https://astrobiology.nasa.gov/news/life-without-the-sun/

129. Danovaro R, Corinaldesi C, Rastelli E, Dell'Anno A. Towards a better quantitative assessment of the relevance of deep-sea viruses, Bacteria and Archaea in the functioning of the ocean seafloor. Aquat Microb Ecol. 2015;75: 81–90. doi:10.3354/ame01747

130. Stetter KO. Smallest Cell Sizes Within Hyperthermophilic Archaea ("Archaebacteria"). National Research Council (US) Steering Group for the Workshop on Size Limits of Very Small Microorganisms. National Academies Press; 1999. Available: https://www.ncbi.nlm.nih.gov/books/NBK224742/

131. Kubo K, Lloyd KG, F Biddle J, Amann R, Teske A, Knittel K. Archaea of the Miscellaneous Crenarchaeotal Group are abundant, diverse and widespread in marine sediments. ISME J. 2012;6: 1949–1965. doi:10.1038/ismej.2012.37

Supplementary Files

This is a list of supplementary files associated with this preprint. Click to download.

- TheSizesofLifeSI2022vers2.pdf